

An X-ray Photoelectron Study of the $(\text{Ca}_{2.5}\text{Th}_{0.5})\text{Zr}_2\text{Fe}_3\text{O}_{12}$, $(\text{Ca}_{1.5}\text{GdTh}_{0.5})(\text{ZrFe})\text{Fe}_3\text{O}_{12}$, and $(\text{Ca}_{2.5}\text{Ce}_{0.5})\text{Zr}_2\text{Fe}_3\text{O}_{12}$ Ceramics with a Garnet Structure

A. Yu. Teterin^a, K. I. Maslakov^a, Yu. A. Teterin^a, L. Vukčević^b, T. S. Livshits^c,
S. V. Yudintsev^c, K. E. Ivanov^a, and M. I. Lapina^c

^a Russian Research Centre Kurchatov Institute, Moscow, Russia

^b Natural Science and Mathematics Faculty, Montenegro University, Podgorica, Montenegro

^c Institute of Geology of Ore Deposits, Petrography, Mineralogy, and Geochemistry,
Russian Academy of Sciences, Moscow, Russia

Received October 30, 2005; in final form, July 16, 2006

Abstract—X-ray photoelectron spectroscopy (XPS) was for the first time applied to examination of the $(\text{Ca}_{2.5}\text{Th}_{0.5})\text{Zr}_2\text{Fe}_3\text{O}_{12}$ (**I**), $(\text{Ca}_{1.5}\text{GdTh}_{0.5})(\text{ZrFe})\text{Fe}_3\text{O}_{12}$ (**II**), and $(\text{Ca}_{2.5}\text{Ce}_{0.5})\text{Zr}_2\text{Fe}_3\text{O}_{12}$ (**III**) ceramics with a garnet structure. The component ratio in the initial charge was set so as to obtain phases with a garnet structure, promising as matrices for immobilization of long-lived actinides. Gadolinium was introduced as a neutron absorber and a simulator of trivalent actinides, Am and Cm. Ceramics **I** and **III** are comprised primarily of a phase with a garnet structure and contain a small amount of oxides with the perovskite and fluorite structures; ceramics **II** consists entirely of a phase with a garnet structure. The oxidation states of the metal ions in the ceramics, as well as the Me–O interatomic distances in the phase structure, were determined by XPS. To this end, both traditional characteristics (line intensities and energy positions) of the X-ray photoelectron spectra of inner electrons and the fine-structure characteristics of the spectra of the valence and inner electrons were used. A change of the composition of the surface of ceramics **II** and **III** upon treatment with 0.01 HCl solution at 150°C and the saturated vapor pressure for 30 days was examined.

PACS numbers: 33.60.Fy, 81.05.Je

DOI: 10.1134/S1066362207010067

Selection of ceramic matrices for long-term storage of radionuclides from high-level waste (HLW) is an important radioecological problem. Information about the speciation (elemental and ionic composition, oxidation state of metals, etc.) of radionuclides and elements in such ceramic matrices facilitates understanding their structure and predicting the processes occurring in them. This allows directed development of materials for long-term storage of various types of HLW and their individual components, above all, rare-earth and actinide elements [1, 2]. X-ray photoelectron spectroscopy (XPS) is an efficient method for examining the speciation of various elements, in particular, lanthanides and actinides, in samples [3, 4]. We applied this method previously to examining the elemental and ionic quantitative compositions and the oxidation state of elements in ferrite- and titanate-based neptunium-containing ceramics [5] as candidate matrices for disposal of long-lived radionuclides of HLW.

Ferrites with a garnet structure are candidate mat-

rices for immobilization of actinide-containing waste [6–8]. In this study, we applied XPS to elemental and ionic analyses of the surface (~5-nm thick) of samples of $(\text{Ca}_{2.5}\text{Th}_{0.5})\text{Zr}_2\text{Fe}_3\text{O}_{12}$ (**I**), $(\text{Ca}_{1.5}\text{GdTh}_{0.5})(\text{ZrFe})\text{Fe}_3\text{O}_{12}$ (**II**), and $(\text{Ca}_{2.5}\text{Ce}_{0.5})\text{Zr}_2\text{Fe}_3\text{O}_{12}$ (**III**) garnet ceramics. We determined the structure of these ceramics and the oxidation state of the metal ions in their composition and also examined the surface composition of ceramics **II** and **III** as influenced by treatment with 0.01 M HCl aqueous solution at 150°C and the saturated vapor pressure for 30 days. These data were analyzed jointly with the results [6–8] of X-ray phase analysis (XPA, DRON-4, CuK_α radiation) and electron microscopic examination with energy-dispersive spectrometry (SEM-EDS: JSM-5300 with a Link ISIS energy-dispersive spectrometer) of the same samples.

EXPERIMENTAL

Ceramics **I–III** were synthesized from the initial mixtures of the oxides whose composition corre-

Binding energies E_b , eV, and line halfwidths Γ ,* eV, of outer (MO) and inner electrons of the garnet ceramics

Sample	MO	Th $4f_{7/2}$	Ca $2p_{3/2}$	Fe $2p_{3/2}$	Gd $4d$ [Ce $4d$]	Gd $3d_{3/2}$ [Ce $4d$]	Zr $3d_{5/2}$	O $1s$
Ia	4.9, 21.3, 24.5, 30.5, 43.3	334.5 (1.1)	346.8 (1.3)	710.7 (3.7), 7.5 sat			182.1 (1.0)	530.2 (1.3), 532.0
IIa	4.9, 8.2, 21.8, 24.4, 30.5, 43.3	334.8 (1.2)	347.1 (1.4)	710.7 (3.9), 7.5 sat	141.4, 143.4, 146.9	1187.2	181.8 (1.0)	530.3 (1.3), 532.5
IIb	6.6, 16.3, 23.3, 29.8	334.2 (1.7)	346.3 (1.4)	710.3 (3.2)	141.2, 143.4, 147.0		181.6 (1.3)	530.3 (1.3), 531.9, 532.6
IIc	3.8, 7.0, 16.6, 21.9, 23.7, 29.8, 43.8	334.2 (1.4)	346.5 (1.5)	710.5 (3.2)	141.2, 143.4, 147.0		181.7 (1.3)	530.3 (1.3), 531.9
IIIa	6.4, 22.1, 25.2, 30.4, 44.3		346.5 (1.5)	710.9 (4.0), 7.9 sat	[108.6], [111.2]	[882.6], 2.6 sat	182.1 (1.1)	530.1 (1.4), 532.4
IIIb	6.4, 22.0, 24.8, 30.5, 43.9		346.5 (1.6)	711.1 (3.9), 7.9 sat	[108.8], [111.7]	[882.6], 3.0 sat	182.4 (1.0)	530.3 (1.3), 532.4
IIIc	4.9, 21.7, 30.5, 45.0			711.1 (4.2), 8.0 sat			182.0 (1.3)	530.0 (1.3), 531.6, 533.1
IIId	4.9, 21.6, 30.7, 44.7			711.1 (4.1), 8.0 sat			182.0 (1.1)	530.0 (1.3), 531.9
Ce $_2$ O $_3$	5.0, 18.0, 36.8				[108.5], [112.0]	[882.3]		
ThO $_2$	5.8, 16.5, 22.0, 25.5	334.3						530.2
Gd $_2$ O $_3$	5.7, 9.0, 22.3, 27.4, 44.3, 48.0				142.8, 147.9	1187.3		529.3
CaO	4.3 (2.1), 20.1 (2.6), 24.3 (2.0), 42.9 (1.9)		346.0 (1.7)					528.9 (1.4)
Fe $_2$ O $_3$	5.4, 7.1, 21.9			711.1 (4.2), 8.0 sat				530.0 (1.3)
ZrO $_2$	5.6, 21.3, 30.6						182.5	530.1

* The line halfwidths in parentheses are referenced to that of the line of the C $1s$ electrons, $\Gamma(C1s) = 1.3$ eV.

sponded to the garnet stoichiometry. They were pressed at 200–400 MPa into pellets 10 mm in diameter and 2–3 mm high. Synthesis was run in an alumina crucible in an oxygen atmosphere in a direct-heating furnace at 1300–1500°C for 3–6 h. The time required for attainment of the equilibrium was 5, 2, and 1 h at 1300, 1400, and 1500°C, respectively.

The X-ray photoelectron spectra of the samples were recorded on an MK II VG Scientific electrostatic spectrometer, using Al K_{α} and Mg K_{α} X-ray radiation in a 1.3×10^{-7} Pa vacuum at room temperature. The resolution of the spectrometer was estimated at 1.2 eV as the halfwidth of the line of Au $4f_{7/2}$ electrons. The electron binding energies E_b , eV, are referenced in this study to that of the C $1s$ electrons of

the hydrocarbons adsorbed on the sample surface, taken equal to 285.0 eV. The electron binding energies and the line halfwidths were measured accurately to within 0.1 eV, and the relative intensities, to 10%. The table lists the halfwidths Γ , eV, of the lines, referenced to $\Gamma(C1s) = 1.3$ eV, which allows comparison with the results of other studies [3, 4]. Samples for recording X-ray photoelectron spectra were prepared from a finely dispersed powder of the initial ceramics, ground in an agate mortar and pressed as dense thick layers into indium on titanium supports or as pellets attached to the support with a two-side scotch tape.

For an XPS examination, the (Ca $_{2.5}$ Th $_{0.5}$)Zr $_2$ ·Fe $_3$ O $_{12}$ (I) ceramics was prepared as a powder (sam-

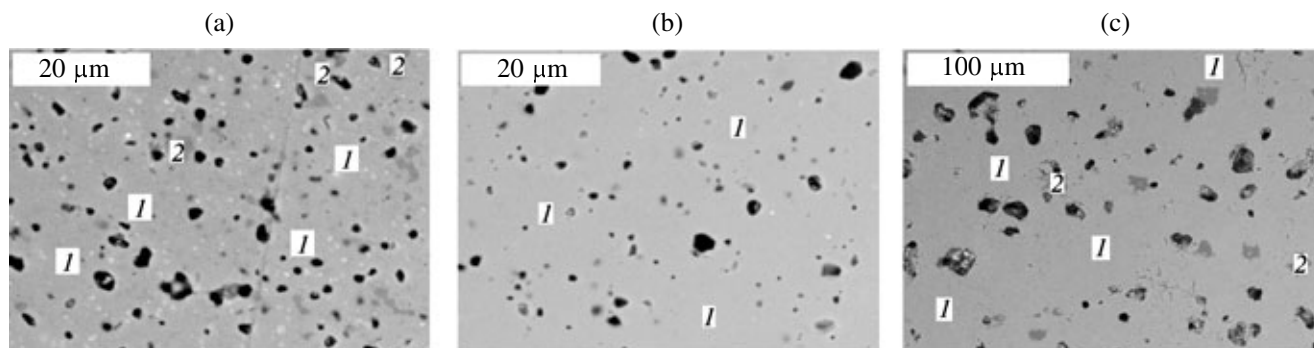


Fig. 1. SEM image (backscattered electron detection) of specimens of ceramics (a) **I**, (b) **II**, and (c) **III**. (I) Phase with a garnet structure and (2) perovskite phase. Black spots are pores. Small white grains in ceramics **I** correspond to thorium oxide (thorianite).

ple Ia). Ceramics $(\text{Ca}_{1.5}\text{GdTh}_{0.5})(\text{ZrFe})\text{Fe}_3\text{O}_{12}$ (**II**) was examined as a powder (sample IIa) and a polished pellet treated with an HCl solution (sample IIb), as well as upon ionic etching for 20 s of the treated pellet surface (sample IIc). Ceramics $(\text{Ca}_{2.5}\text{Ce}_{0.5})\text{Zr}_2\text{Fe}_3\text{O}_{12}$ (**III**) was examined as a powder (sample IIIa), a polished pellet (sample IIIb), and unpolished pellet treated with an HCl solution (sample IIIc), as well as upon ionic etching for 40 s of the treated pellet surface (sample IIId).

The pellets were treated with 0.01 M aqueous HCl solution at 150°C and the saturated vapor pressure for 30 days. Ionic etching of the surface was carried out with Ar^+ ions directly in the spectrometer chamber at $I = 30 \mu\text{A}$ ($j = 5 \mu\text{A cm}^{-2}$), $U = 1 \text{ kV}$ (etching rate V for SiO_2 is 2 \AA min^{-1}).

All the samples were subjected to atomic and ionic quantitative analyses, based on the fact that the spectral line intensity is proportional to the concentration of the ions in the sample of interest. In this study, such analysis was based on the relationship $n_i/n_j = (S_i/S_j)/(k_j/k_i)$, where n_i/n_j is the relative concentration of the atoms examined; S_i/S_j , relative intensity (area) of the line of electrons of inner shells of these atoms; and k_j/k_i , experimental relative sensitivity coefficient. In this study, we used the following coefficients referenced to carbon: 1.00 (C1s), 2.64 (O1s), 4.2 ($\text{Ca}2p_{3/2}$), 6.32 ($\text{Ca}2p$), 8.4 (Zr3d), 4.16 ($\text{Zr}3p_{3/2}$), 12 ($\text{Fe}2p$), 8 ($\text{Fe}2p_{3/2}$), 1.04 ($\text{Fe}3p$), 12 ($\text{Gd}3d_{5/2}$), 8.0 ($\text{Gd}4d$), 31.2 ($\text{Th}4f_{7/2}$), 3.6 ($\text{Th}5d_{5/2}$), 24.0 ($\text{Ce}3d_{5/2}$), and 8.0 ($\text{Ce}4d$) [9]. Interpretation of the X-ray photoelectron spectra of the samples was based on the characteristics of the spectra of CaO , Fe_2O_3 , ThO_2 , Gd_2O_3 , Ce_2O_3 , and ZrO_2 (see table).

RESULTS AND DISCUSSION

Ceramics with a garnet structure. This structure can be described by the formula $\text{VIII A}_3 \text{VI B}_2 \text{IV X}_3 \text{O}_{12}$ (space group $la3d$ of the hexahedral symmetry class O_h^{10} , $Z = 8$). It consists of a three-dimensional skeleton of alternating XO_4 tetrahedra and BO_6 octahedra sharing common vertices. The voids shaped as distorted cubes (trigonal dodecahedra) are occupied by large anions. Three structural positions, A, B, and X with the coordination numbers 8, 6, and 4, respectively, allow incorporation of various elements into the garnet lattice. The VIII A position is typically occupied by bi- (Ca^{2+} , Fe^{2+}) and trivalent (La^{3+} , Gd^{3+} , Ce^{3+}) cations. The VI B positions are occupied by tri- (Fe^{3+}) and tetravalent (Zr^{4+}) ions, and the IV X position, by tri- (Fe^{3+}) and tetravalent (Si^{4+}) cations [2, 10]. The XPS and SEM-EDS data we obtained suggest that, in ceramics **I**, the garnet phase is dominating, and traces of phases with perovskite (a composition close to CaZrO_3) and fluorite (ThO_2 , thorianite) structures are also present; ceramics **II** consists solely of a garnet phase, and ceramics **III** is comprised of the dominating target garnet phase and a minor amount of calcium zirconate with a perovskite structure (Fig. 1).

X-ray photoelectron spectra. The X-ray photoelectron spectra of samples of the ceramics at the electron binding energies within 0–1000 eV contain lines corresponding to their constituting elements. This energy range can be conventionally divided into three narrower ranges [3, 4]. The first range, 0–15 eV, exhibits a structure associated mainly with electrons from the outer valence molecular orbitals (OVMOs) formed mostly by electrons of unfilled valence atomic shells. The second energy range, 15–50 eV, exhibits a structure associated mostly with the electrons from

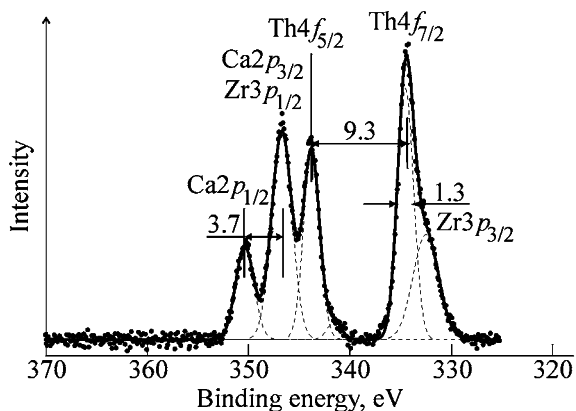


Fig. 2. X-ray photoelectron spectra of Th4f, Zr3p, and Ca2p electrons of sample Ia of garnet ceramics.

inner valence MOs (IVMOs) and from low-energy completely filled valence shells of the neighboring atoms. This pattern characterizes the composition of the nearest surrounding of the ion in the compound. In particular, for actinides the parameters of this spectral pattern can be used for estimating the length of the bond linking the central actinide atom with its nearest neighbors [3, 4]. The third range, from 50 eV and over, exhibits a structure of the spectrum of inner electrons weakly involved in formation of inner (core) MOs, which is virtually neglected in discussion of the X-ray photoelectron spectra. However, this part may contain a structure originating from spin-orbital coupling with the splitting ΔE_{sl} , eV, the multiplet splitting ΔE_{ms} , eV, the multielectron excitation ΔE_{sat} , eV, dynamic effect, etc. Since the parameters of such a structure characterize different properties of compounds, they are used in combination with such conventional characteristics as electron binding energy, chemical shifts of the levels and interlevel distances, and the spectral line intensity [3]. To simplify further discussion, we will use both molecular and atomic terms and designations.

Spectra of low-energy electrons (0–50 eV). The low-energy part of the spectra of the garnets contains a structure associated with Ca4s, Th6d, 7s, Zr4d, 5s, Fe3d, 4s, Gd4f, 5d, 6s, Ce4f, 5d, 6s, and O2p OVMO electrons, as well as a structure associated with Ca3s, 3p, Th6s, 6p, Zr4p, Gd5s, 5p, Ce5s, 5p, and O2s IVMOs (see table). An intense maximum at 8.2 eV corresponding to Gd4f electrons is observed in the spectrum of the OVMO electrons of sample Iia (see table). In the region corresponding to the spectra of the IVMO electrons (sample Iia), the most prominent are the maxima near the binding energies of Ca3p and Ca3s electrons at 24.4 and 43.3 eV, as well as

the maxima at the binding energies of Zr4p (30.1 eV) and O21s (21.8 eV) electrons. Upon treatment of the surface of ceramics II with an acid solution (samples Iib, Iic), the line of Gd4f and Ca3s, 3p electrons substantially decreased in intensity relative to that of Zr4p electrons, which is due to removal of these elements from the sample surface. Surface etching of this sample with argon ions does not substantially change the spectra. The spectrum of sample IIIa contains, along with the lines typical for the compounds of interest, small maxima at 10 and 13 eV, evidently, due to the presence on the surface of a minor impurity of the CO_3^{2-} groups, whose structure is also observed in the spectra of the C1s electrons of hydrocarbons adsorbed on the surface. Upon treatment of the surface of ceramics III with an acid solution, the line of the Ca3p electrons virtually disappears; a line observed at 45 eV belongs to the X-ray $K_{\alpha_{3,4}}$ satellite of the intense line of the Fe3p electrons at 55 eV. Unfortunately, the structure of these spectra allows only qualitative elemental analysis, since these spectra consist of lines reflecting, essentially, systems of molecular orbitals, rather than of individual atomic lines. In most cases, the spectra in this segment contain only lines typical for the compounds of interest.

Spectra of inner electrons (50–1000 eV). Elemental and ionic quantitative analyses of the samples by XPS typically utilize the most intense lines of their constituting elements [9, 11]. At the same time, important characteristics for determining the oxidation state of transition elements M3d, Ln4f, and An5f (M is metal; Ln, lanthanide; and An, actinide) are also the fine-structure parameters of the lines. For example, the structure of the shake-up satellite of the Fe2p, Ln3d, and An4f electrons allows estimating the oxidation state of the ion and the extent of the bond ionicity [3, 4].

For the ceramics of interest, we selected lines of Ca3s, 2p, Fe3s, 3p, 2p, Th4f, 5d, Zr3p, 3d, Gd4d, 3d, Ce4d, 3d, and O1s electrons (see table, Figs. 2–7). Unfortunately, we could not obtain reliable spectra in all cases because of a low intensity of the line of Mns electrons. When the spectra of different elements overlap, like in the case of the lines associated with Th4f, Zr3p, and Ca2p electrons (Fig. 2), other, better resolved, lines can be used, e.g., that of Zr3d electrons. The spectra of Th4f, Zr3p, and Ca2p electrons are observed as characteristic doublets due to spin-orbital coupling with the ΔE_{sl} splittings of 9.3 eV for Th4f, 13.7 eV for Zr3p, and 3.5 eV for Ca2p electrons [12]. It should be noted that the binding energies of the Ca2p_{3/2} and Zr3p_{1/2} electrons are virtually identical

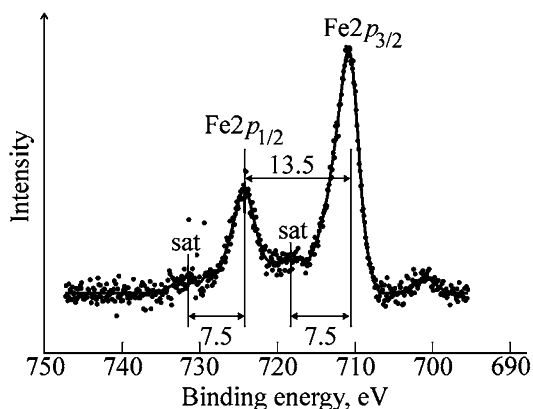


Fig. 3. X-ray photoelectron spectra of Fe2p electrons of sample IIa of garnet ceramics.

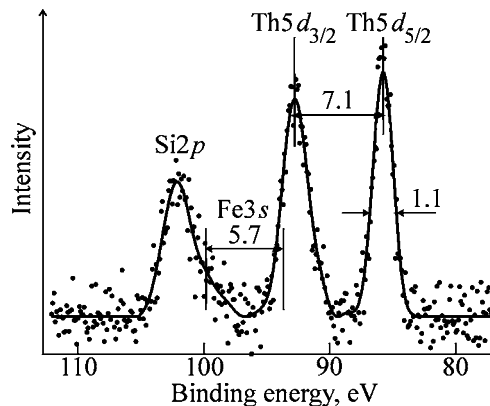


Fig. 4. X-ray photoelectron spectra of Th5d and Fe3s electrons of sample Ia of garnet ceramics.

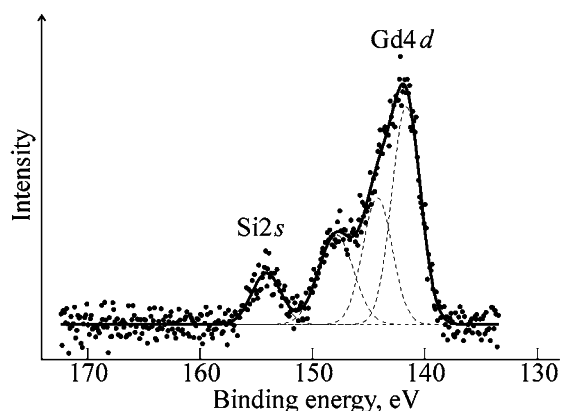


Fig. 5. X-ray photoelectron spectra of Gd4d electrons of sample IIa of garnet ceramics.

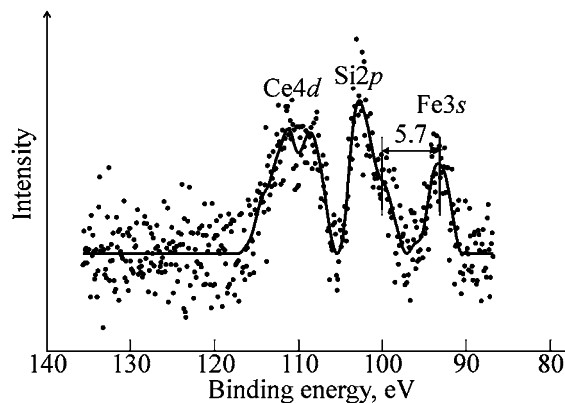


Fig. 6. X-ray photoelectron spectra of Ce4d and Fe3s electrons of sample IIIa of garnet ceramics.

ical (Fig. 2). Upon treating ceramics **II** with an acid solution, the relative intensity of the lines of the Ca2p electrons in the X-ray photoelectron spectra of samples IIb and IIc significantly decreased, and for ceramics **III** upon such a treatment the doublet of the Ca2p electrons almost completely disappeared (samples IIIc and IIIId).

The spectra of the C1s electrons of samples Ia and IIa are fairly symmetrical; they exhibit weak peaks associated with the Th4s electrons from the high electron binding energy side and, possibly, electrons of the CO_3^{2-} carbonate group at 288.8 eV. Upon treating ceramics **II** with an acid solution, this spectrum exhibits an additional weak line at 286.8 eV, which can be assigned to the carbon atoms of the carbonyl ($>\text{C}=\text{O}$) group. This line disappears upon treating the surface with argon ions (sample IIc). The spectra of the C1s electrons of ceramics **III** have a complex structure. Sample IIIa, along with the main line associated with the hydrocarbons on its surface, exhibits

an additional line at 288.9 eV. It is associated both with the carbon from the carbonate group (CO_3^{2-}) and the Ce4s electrons. The spectrum of the C1s electrons of sample IIIc treated with an acid solution consists

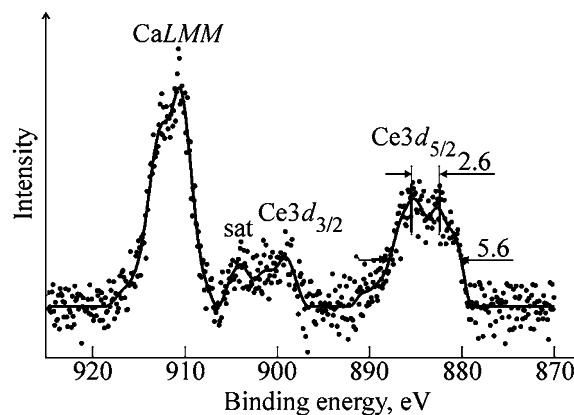


Fig. 7. X-ray photoelectron spectra of Ce3d electrons of sample IIIa of garnet ceramics (MgK_{α} exciting radiation).

primarily of three lines, at 285.0, 286.6, and 288.3 eV. They can be assigned to the surface carbons of saturated hydrocarbons and carbonyl ($>C=O$) and carbonate (CO_3^{2-}) groups, respectively. Upon treatment of the surface of this sample with argon ions, the spectrum exhibits the main line at 285.0 eV and a weak shoulder at 288.2 eV. This suggests that brief etching of the surface with argon ions resulted in virtually complete removal of the carbonyl ($>C=O$) and carbonate (CO_3^{2-}) groups, as well as of nearly a half of the saturated hydrocarbons.

The spectrum of the Fe2*p* electrons of sample IIa consists of the spin-doublet [$\Delta E_{s1}(Fe2p) = 13.5$ eV, $G(Fe2p_{3/2}) = 2.5$ eV] and contains a weak shake-up satellite [$\Delta E_{sat}(Fe2p_{3/2}) = 7.5$ eV] from the higher electron binding energy side of the main line (Fig. 3). The line of the Fe3*p* electrons of this garnet is manifested as a single line: $E_b(Fe3p) = 55.4$ eV, $G(Fe3p) = 1.9$ eV. Similar spectra with close binding energies (see table) are also observed for all the other samples of the ceramics. The binding energy of the Fe2*p* electrons and the structure of the shake-up satellites suggest that the iron ions are in the oxidation state of 3+. Indeed, the $E_b(Fe2p_{3/2})$, $\Delta E_{sat}(Fe2p_{3/2})$, and $E_b(Fe3p)$ parameters for Fe₂O₃ were estimated at 711.4, 8, and 56.4 eV [13], respectively; $\Delta E_{sat} = 7.1$ eV [14]; 711.1, 8.0, and 56 eV [15], respectively; and for FeO, 709.7, 6, and 54.9 eV [13]; $\Delta E_{sat} = 6.1$ eV [14]; 710.3 and 5.6 eV [15], respectively. Upon treatment of ceramics II with an acid solution, the relative intensity of the line of the Fe2*p* electrons decreased by a factor of approximately 6.

In the region of the spectra of the Th5*d* electrons in samples of ceramics I and II (Fig. 4), the low-energy component of the spin-doublet in the spectrum of the Th5*d*_{3/2} electrons overlaps with the spectrum of the Fe3*s* electrons. Also, a line corresponding to the Si2*p* electrons of the impurity Si that got into the sample during grinding is observed (this line is lacking in the spectra of the pellets of samples IIa and IIb). The line of the Si2*p* electrons can overlap with the low-energy component of the structure of the spectrum of the Fe3*s* electrons, caused by the multiplet splitting (Fig. 4). Indeed, from the lower binding energy side of the line of the Si2*s* electrons there is a shoulder separated from the line of the Th5*d*_{3/2} electrons by 5.7 eV (the multiplet splitting of the line of the Fe3*s* electrons for Fe³⁺). However, the structure in this region can be due also to the satellites from the lines of the Th4*d* electrons. Thus, the Fe3*s* line is unsuitable for unambiguous determination of oxidation state of the Fe ions.

The Gd4*d* electrons of ceramics II exhibit a spectrum typical for the Gd³⁺ ion (Fig. 5) [4]. An additional line at 153.7 eV can be partially associated with the Si2*s* electrons of the impurity Si. At first glance, the spectrum of the Gd4*d* electrons is a doublet due to the spin-orbital coupling. However, this is not the case. The Gd³⁺ ion contains seven unpaired Gd4*f* electrons, which is responsible for an extremely complex shape of the line of Gd4*d* electrons, extending for 40 eV, due to multiplet splitting [4]. Despite the fact that identification of this structure is a difficult task, the structure proper is suitable for determination of the oxidation state of the gadolinium ion at the "fingerprint" level. The binding energy of the Gd3*d*_{5/2} electrons is 1187.2 eV, which also characterizes the oxidation state of Gd³⁺.

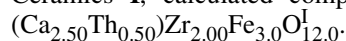
A complex structure is observed in the region of the spectrum of the Ce4*d* electrons of sample IIIa (Fig. 6). Two low-energy lines at 93.3 and 99.0 eV are associated with Fe3*s* electrons, whose spectrum, to a first approximation, is a doublet due to multiplet splitting with $\Delta E_{ms}(Fe3s) = 5.7$ eV. Also, this doublet overlaps with the line at 102.8 eV, associated with the impurity Si atoms that got into the sample during grinding. The spectrum of the Ce4*d* electrons of sample IIIa (Fig. 6) has a complex structure with two maxima at 108.6 and 111.2 eV, which is typical for Ce³⁺ ions [14]. In the same region, the spectrum of sample IIIc treated with an acid solution exhibits only a relatively intense spectrum of the Fe3*s* electrons with $\Delta E_{ms}(Fe3s) = 6.1$ eV and the line of Ce4*d* electrons is virtually lacking. Treatment with argon ions for 40 s does not change this spectrum. These data suggest that, upon treatment with an acid solution, Ce is virtually completely washed off from the ceramics surface.

In the region of the X-ray photoelectron spectra of the Ce3*d* electrons of ceramics III, recorded using AlK_α exciting radiation, an intense spectrum of the FeLMM Auger electrons prevented identification of the lines of Ce3*d* electrons. Therefore, we recorded the X-ray photoelectron spectra of the Ce3*d* electrons using MgK_α exciting irradiation (Fig. 7). In this case, the spectrum of the Ce3*d* electrons of sample IIIa consists of a spin-doublet with $\Delta E_{s1}(Ce3d) = 18.3$ eV, $\Gamma(Ce3d_{5/2}) = 2.0$ eV and a shake-up satellite on the high binding energy side from the main lines of the doublet, with $\Delta E_{sat}(Ce3d_{5/2}) = 2.6$ eV and relative intensity $I_{sat}/I_0 = 65\%$ (Fig. 7; see table). This spectrum is characteristic for the Ce³⁺ ions. Upon treatment of the ceramics with an acid solution, the line of the Ce3*d* electrons disappears in the spectral region of

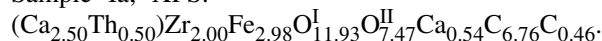
interest. This agrees with the data derived from the structure of the spectrum of the Ce4d electrons.

Quantitative elemental and ionic analyses. Based on the line intensities (areas), taking into account the experimental XPS sensitivity coefficients, we determined the relative atomic composition of the surface of the examined samples of ceramics I–III. Also, for comparison we presented the calculated composition of the ceramics and the bulk composition of the ceramics according to the SEM-EDS data. Different indices in the designations of the oxygen atoms correspond to different chemical states of oxygen: ^I refers to metal-bound oxygen, and ^{II}, ^{III}, to oxygen in the composition of hydroxide, carbonate, or other groups on the sample surface.

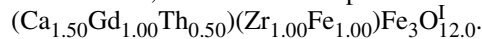
Ceramics I, calculated composition:



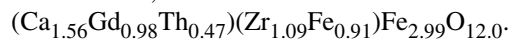
Ceramics I, SEM-EDS: $(\text{Ca}_{2.57}\text{Th}_{0.49})\text{Zr}_{2.02}\text{Fe}_{2.94}\text{O}_{12.0}$
Sample Ia, XPS:



Ceramics II, calculated composition:



Ceramics II, SEM-EDS:

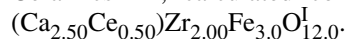


Sample IIa, XPS: $(\text{Ca}_{1.50}\text{Gd}_{1.00}\text{Th}_{0.54})(\text{Zr}_{1.00}\text{Fe}_{1.00})\cdot$
 $\text{Fe}_{2.67}\text{O}_{11.59}^{\text{I}}\text{O}_{11.12}^{\text{II}}\text{Ca}_{0.98}\text{C}_{5.87}\text{C}_{1.16}$

Sample IIb, XPS: $(\text{Ca}_{0.59}\text{Gd}_{0.23}\text{Th}_{0.32})(\text{Zr}_{1.00}\text{Fe}_{0.61})\cdot$
 $\text{Fe}_{0.00}\text{O}_{3.44}^{\text{I}}\text{O}_{4.97}^{\text{II}}\text{O}_{0.97}^{\text{III}}\text{C}_{5.87}\text{C}_{1.16}$

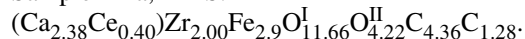
Sample IIc, XPS: $(\text{Ca}_{0.79}\text{Gd}_{0.19}\text{Th}_{0.32})(\text{Zr}_{1.00}\text{Fe}_{0.62})\cdot$
 $\text{Fe}_{0.00}\text{O}_{3.44}^{\text{I}}\text{O}_{3.74}^{\text{II}}\text{O}_{0.97}^{\text{III}}\text{C}_{5.91}\text{C}_{1.01}$

Ceramics III, calculated composition:

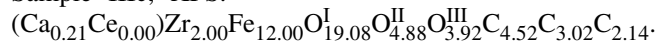


Ceramics III, SEM-EDS: $(\text{Ca}_{2.53}\text{Ce}_{0.52})\text{Zr}_{1.96}(\text{Fe}_{3.01})\text{O}_{12.0}$

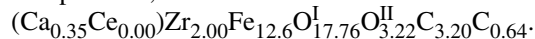
Sample IIIa, XPS:



Sample IIIc, XPS:



Sample IIIId, XPS:



The composition of the surface of samples Ia, IIa, and IIIa, determined from the characteristics of the X-ray photoelectron spectra, differ slightly from that calculated and derived from the SEM-EDS data. One of the main reasons is that XPS is a surface-sensitive method. The error in measuring the areas of the lines in the X-ray photoelectron spectra increases for low concentrations of the elements (the sensitivity of the method is ~0.1–1.0 wt % of the substance). The increased content of calcium, revealed by the XPS analysis, is evidently due to its migration to the sample

surface and formation of calcium hydroxides and/or carbonates.

Upon treatment of ceramics II with an acid solution, the content of Ca on its surface decreased by a factor of ca. 3, that of Fe, by a factor of 6, that of Gd, by a factor 5, and that of Th, by half relative to Zr. Subsequent etching of the surface of this sample with argon ions did not significantly change the composition of the surface (sample IIc), except for the content of Ca. Upon treatment of ceramics III with an acid solution, the content of Ca on its surface relative to Zr decreased more than tenfold, Ce was lacking, and the amount of Fe increased more than fourfold.

Determination of the metal–oxygen bond length.

The spectra of the O1s electrons of the ceramics examined consist of two lines at 530.2 and 532.3 eV (sample Ia), at 530.3 and 532.5 eV (sample IIa), and at 530.1 and 532.4 eV (sample IIIa). The equation

$$E_b \text{ (eV)} = 2.27(R_{\text{M-O}})^{-1} \text{ (nm)} + 519.4$$

derived in [16] allows estimation of the metal–oxygen distances $R_{\text{M-O}}$, nm, in the samples examined from the binding energies of the O1s electrons. These parameters were estimated at 0.210 and 0.176 nm (sample Ia); 0.208 and 0.173 nm (sample IIa); and 0.212 and 0.175 nm (sample IIIa).

The above-mentioned equation suggests that, with increasing $R_{\text{M-O}}$, the binding energy of the O1s electrons tends to decrease. Apparently, the distances of 0.173–0.176 nm are too short to be observed in the ceramics proper; they can be assigned to hydroxide and/or carbonate groups on the surface [11]. This is also consistent with the elemental analysis data, which suggest that the O1s electrons of oxygen in the ceramics samples examined have virtually identical binding energies. Treatment of ceramics II with an acid solution substantially modifies the structure of the spectrum of the O1s electrons: The high-energy component increases in intensity; a third component appears on the higher electron binding energy side and disappears after etching the sample with argon ions.

Thus, the ceramics samples with the empirical formulas $(\text{Ca}_{2.5}\text{Th}_{0.5})\text{Zr}_2\text{Fe}_3\text{O}_{12}$ (I), $(\text{Ca}_{1.5}\text{GdTh}_{0.5})\cdot(\text{ZrFe})\text{Fe}_3\text{O}_{12}$ (II), and $(\text{Ca}_{2.5}\text{Ce}_{0.5})\text{Zr}_2\text{Fe}_3\text{O}_{12}$ (III), constituted by the dominating garnet phase, were examined by X-ray photoelectron spectroscopy. Based on characteristics of the spectra of the outer and inner electrons from the binding energy range 0–1000 eV, quantitative elemental and ionic analyses were carried out. As expected, the oxidation state of the metal ions

in this ceramics corresponded to the Ca^{2+} , Fe^{3+} , Zr^{4+} , Gd^{3+} , Ce^{3+} , and Th^{4+} ions.

The binding energies of the oxygen electrons suggest that the oxygen ions in the garnet ceramics examined occur in chemically equivalent states. The metal–oxygen bond lengths in the garnets examined were estimated at 0.210 (I), 0.208 (II), and 0.212 (III) nm.

Upon treatment of ceramics II with an aqueous 0.01 M HCl solution at 150°C for 30 days, the content of Ca relative to Zr on its surface decreased approximately threefold, that of Fe, sixfold, that of Gd, fivefold, and that of Th, by half. Upon identical treatment of ceramics III, the content of Ca on the surface decreased relative to Zr more than tenfold, Ce was lacking, and the amount of Fe increased more than fourfold.

ACKNOWLEDGMENTS

This study was financially supported by the Russian Foundation for Basic Research (projects nos. 04-03-32892 and 05-05-64005) and the State Program of Support for Leading Scientific Schools of the Russian Federation (grant no. NSh-284.2006.3).

REFERENCES

- Laverov, N.P., Yudintsev, S.V., Stefanovsky, S.V., et al., *Mater. Res. Soc. Symp. Proc.*, 2002, vol. 713, pp. 337–344.
- Laverov, N.P., Yudintsev, S.V., Yudintseva, T.S., et al., *Geol. Rudn. Mestorozhd.*, 2003, vol. 45, no. 6, pp. 483–513.
- Teterin, Yu.A. and Teterin, A.Yu., *Usp. Khim.*, 2004, vol. 73, no. 6, pp. 588–631.
- Teterin, Yu.A. and Teterin, A.Yu., *Usp. Khim.*, 2002, vol. 71, no. 5, pp. 403–441.
- Teterin, Yu.A., Maslakov, K.I., Vukcevic, L., et al., Abstracts of Papers, *7th Int. Conf. "Actinides 2005"*, Manchester (the United Kingdom), July, 2005, 6P23, p. 168.
- Yudintsev, S.V., *Geol. Rudn. Mestorozhd.*, 2003, vol. 45, no. 2, pp. 172–187.
- Yudintseva, T.S., *Geol. Rudn. Mestorozhd.*, 2005, vol. 47, no. 5, pp. 444–450.
- Yudintsev, S.V., Osherova, A.A., and Dubinin, A.V., *Mater. Res. Soc. Symp. Proc.*, 2004, vol. 824, pp. 287–292.
- Practical Surface Analysis by Auger and X-ray Photoelectron Spectroscopy*, Briggs, D. and Seah, M.P., Eds., New York: Wiley, 1983.
- Wells, A., *Structural Inorganic Chemistry*, Oxford: Oxford Univ. Press, 1986, vols. 2–3.
- Nefedov, V.I., *Rentgenoelektronnaya spektroskopiya khimicheskikh soedinenii* (X-ray Photoelectron Spectroscopy of Chemical Compounds), Moscow: Khimiya, 1984.
- Fuggle, J.C. and Martensson, N., *J. Electron Spectrosc. Relat. Phenom.*, 1980, vol. 21, pp. 275–281.
- Mills, P. and Sullivan, J.L., *J. Phys. D: Appl. Phys.* 1983, vol. 16, pp. 723–732.
- Zimmermann, R., Steiner, P., Claessen, R., et al., *J. Phys. F: Condens. Matter*, 1999, vol. 11, pp. 1657–1682.
- Descostes, M., Mercier, F., Thromat, N., et al., *Appl. Surf. Sci.*, 2000, vol. 165, pp. 288–302.
- Sosul'nikov, M.I. and Teterin, Yu.A., *Dokl. Akad. Nauk SSSR*, 1991, vol. 317, no. 2, pp. 418–421.